Study on the optical mechanism of resist-photorefractive Zr-doped lithium niobate crystals from first-principle calculations

Electronic Supplementary Material

Weiwei Wang[a], Hongde Liu*[b], Dahuai Zheng[b], Yue Liu[c], Yongfa Kong*[b], Jingjun Xu[b]

a. Department of Mathematics and Physics, Shijiazhuang Tiedao University, Shijiazhuang 050043, China.
b. MOE Key Laboratory of Weak-Light Nonlinear Photonics, TEDA Institute of Applied Physics and School of Physics, Nankai University, Tianjin 300457, China. Email:liuhd97@nankai.edu.cn; kongyf@nankai.edu.cn;
c. College of materials Science and Engineering, Liaoning Technical University, Liaoning 123032, China

1. The test of k-points.

We tested the energy and convergence of different k-points with the lithium niobate supercell including 120 atoms. The results are displayed in the following figure S1.

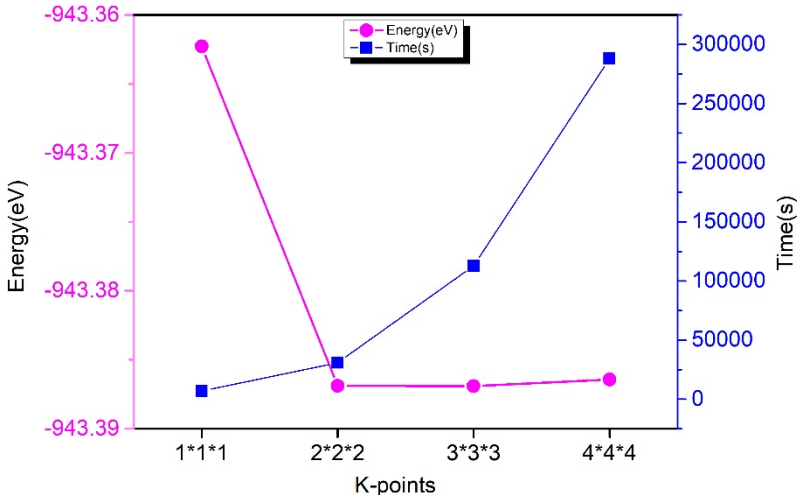

Figure S1. The energy and convergence of different k-points with the lithium niobate supercell.

As shown in the figure S1, the energy changes with the variation of k-point sampling. When k-point adopts 2×2×2 mesh, the energy reaches its lowest value, while

when k-point is 4×4×4, the energy increases. Moreover, it can be seen from the pictures that the time required for structural convergence increases with the increase of the number of k-points. Combining the energy convergence situation and the time required for the convergence of lithium niobate results, using a 2×2×2 k-point mesh is the most suitable.

2. The test of lithium niobate supercell.

There have been many literature reports on the study of the lattice constant of lithium niobate crystals. We have listed several lattice structures of lithium niobate we used in Table S1. The structure is a hexagonal crystal cell containing 30 atoms (6 Li atoms, 6 Nb atoms, and 18 O atoms).

Table S1. Lattice structures of lithium niobate.

a=b (Å)	c(Å)	volume	α(◦)	β(◦)	γ(◦)
5.185	13.990	325.781 Å^3	90	90	120

We expanded the original cell of lithium niobate to 2×1×1, 2×2×1 and 2×2×2 supercell. The supercells were simulated and tested separately. As we can see from the figure S2, the band structures of 2×2×1 supercell and 2×2×2 supercell are basically the same, the bandgap are 3.57 eV and 3.58 eV respectively, and the difference in bandgap values is not significant. The supercell of 2×2×1 can meet the construction of defect models. Taking into account existing calculation conditions and other relevant factors, the supercell used in this paper is 2×2×1 supercell, which contains 120 atoms (24 Li atoms, 24 Nb atoms, and 72 O atoms).

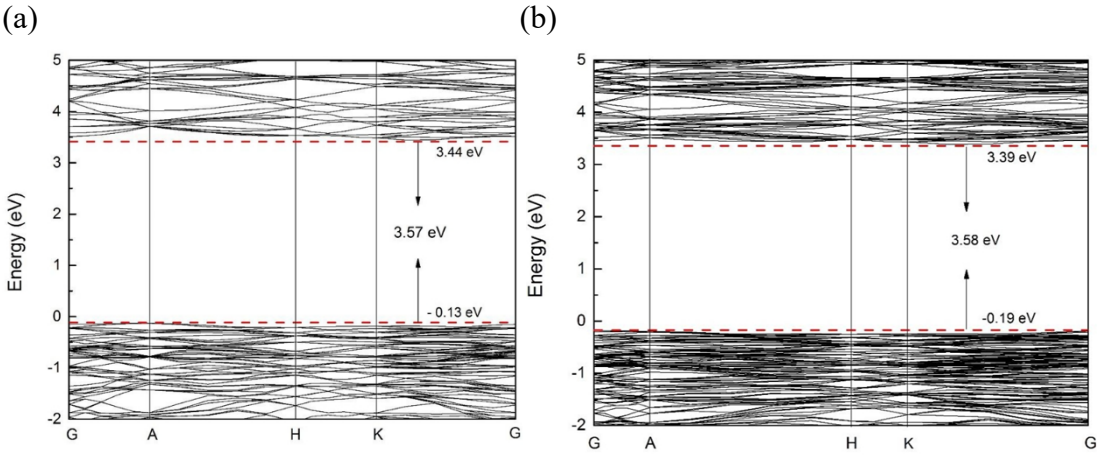

Figure S2. (a) and (b) are the band structure calculated with 2×2×1 supercell and 2×2×2 supercell, respectively.

3. The calculation of defect formation energy

Generally, DFEs of a defect or defects X with charge q can be calculated as

$$\Delta E_f(X^q) = E^{total}(X^q) - E^{total}(\text{perfect}) + \sum_i n_i u_i + q(E_f + E_v + \Delta V) \quad (1)$$

From this, we can determine the intrinsic defects such as Nb-antisite and lithium vacancies, as well as the stable charge states of doped ions in lithium niobate. We use lithium vacancies as an example to illustrate the specific calculation process. The defect formation energies of v_{Li}^{-} and v_{Li}^{0} are listed in the Table S2, Table S3 and figure S3.

Table S2. The defect formation energy of v_{Li}^{-}.

ΔE_f	$E_{f/\text{eV}}$	$E^{total}(vLi)$/eV	E(perfect)/eV	n_{Li}	$u_{Li/\text{eV}}$	q	$E_{v/\text{eV}}$	ΔV/eV
3.55504	0	-948.315563	-958.313201	1	-3.34	-1	3.0906	0.012
3.05504	0.5	-948.315563	-958.313201	1	-3.34	-1	3.0906	0.012
2.55504	1	-948.315563	-958.313201	1	-3.34	-1	3.0906	0.012
2.05504	1.5	-948.315563	-958.313201	1	-3.34	-1	3.0906	0.012
1.55504	2	-948.315563	-958.313201	1	-3.34	-1	3.0906	0.012
1.05504	2.5	-948.315563	-958.313201	1	-3.34	-1	3.0906	0.012
0.55504	3	-948.315563	-958.313201	1	-3.34	-1	3.0906	0.012
0.05504	3.5	-948.315563	-958.313201	1	-3.34	-1	3.0906	0.012
-0.44496	4	-948.315563	-958.313201	1	-3.34	-1	3.0906	0.012
-0.94496	4.5	-948.315563	-958.313201	1	-3.34	-1	3.0906	0.012
-1.44496	5	-948.315563	-958.313201	1	-3.34	-1	3.0906	0.012

Table S3. The defect formation energy of v_{Li}^{0}.

ΔE_f	$E_{f/\text{eV}}$	$E^{total}(vLi)$/eV	E(perfect)/eV	n_{Li}	$u_{Li/\text{eV}}$	q	$E_{v/\text{eV}}$	ΔV/eV
3.61743	0	-951.355762	-958.313201	1	-3.34	0	3.0906	0.087
3.61743	0.5	-951.355762	-958.313201	1	-3.34	0	3.0906	0.087
3.61743	1	-951.355762	-958.313201	1	-3.34	0	3.0906	0.087
3.61743	1.5	-951.355762	-958.313201	1	-3.34	0	3.0906	0.087
3.61743	2	-951.355762	-958.313201	1	-3.34	0	3.0906	0.087
3.61743	2.5	-951.355762	-958.313201	1	-3.34	0	3.0906	0.087
3.61743	3	-951.355762	-958.313201	1	-3.34	0	3.0906	0.087
3.61743	3.5	-951.355762	-958.313201	1	-3.34	0	3.0906	0.087
3.61743	4	-951.355762	-958.313201	1	-3.34	0	3.0906	0.087
3.61743	4.5	-951.355762	-958.313201	1	-3.34	0	3.0906	0.087
3.61743	5	-948.315563	-958.313201	1	-3.34	-1	3.0906	0.087

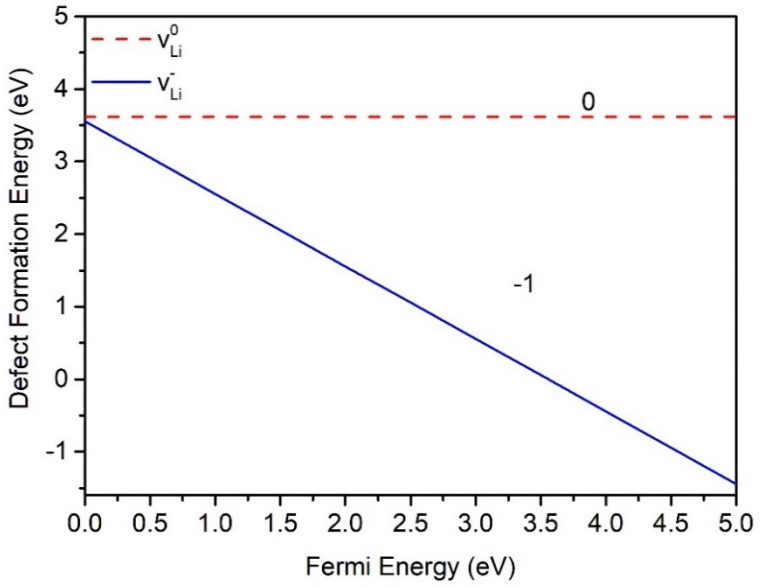

Figure S3. The defect formation energies of v_{Li}^- and v_{Li}^0 with the change of Fermi energy.

The figure S3 show the formation energies of v_{Li}^- and v_{Li}^0 with the increase of Fermi energy. From the it, we can see that the formation energy of v_{Li}^0 is higher than the formation energy of v_{Li}^- at any Fermi energy. It is indicated that the v_{Li}^- is more stable than v_{Li}^0 in lithium niobate. Using the same methods, we can obtain the stable charge states of Nb-antisite as 0, +2, +4, which vary with the Fermi energy. Similarly, the stable charge states of Zr_{Li} are 0 and +3, and the stable charge state of Zr_{Nb} is -1. The transfer energies of these point defects are list in the table S4.

Table S4. The transfer energies of different point defects with different stable charge state.

Point defects	Transfer Point	Transfer Energy (eV)
Nb_{Li}	CBM/0	7.32
	0/+2	3.4
	+2/+4	3.09
	+4/VBM	-5.67
Zr_{Li}	CBM/0	5.89
	0/+3	3.65
	+3/VBM	-5.02
Zr_{Nb}	-1/VBM	1.62
	-1/CBM	-3.12
v_{Li}	-1/VBM	3.56
	-1/CBM	-1.44

4. The calculation of refractive index.

The refractive index can be obtained through the following formula,

$$\varepsilon(\omega)=\varepsilon_1(\omega)+ i\varepsilon_2(\omega) \quad (2)$$

$$n=\left(\frac{\sqrt{\varepsilon_1^2+\varepsilon_2^2}+\varepsilon_1}{2}\right)^{\frac{1}{2}} \quad (3)$$

Where $\varepsilon(\omega)$ is the dielectric function which can be obtained from the optical properties calculation, and $\varepsilon_1(\omega)$ is the imaginary part and $\varepsilon_2(\omega)$ is the real part of the dielectric function, and ω is the Photon frequency. The refractive indices of the ordinary (o) and extraordinary (e) light of pure $LiNbO_3$ crystals and $LiNbO_3$ with defect clusters: $Zr_{Li}^{3+}+Nb_{Li}^{4+}+7v_{Li}^{-}$, $Zr_{Li}^{3+}+3v_{Li}^{-}$, $Zr_{Li}^{3+}+3Zr_{Nb}^{-}$, $2Zr_{Li}^{3+}+3Zr_{Nb}^{-}+3v_{Li}^{-}$, are listed in the Table S5. At the same time, the birefringence of them is also listed in the Table S5.

Table S5. The refractive indices and birefringence of pure $LiNbO_3$ and $LiNbO_3$ with defect clusters: calculated at the wavelength λ = 1064 nm and 1550 nm.

Defect cluster	**Refractive index**					
	wavelength 1064 nm			**wavelength 1550 nm**		
	$\mathbf{n_o}$	$\mathbf{n_e}$	$\mathbf{n_e-n_o}$	$\mathbf{n_o}$	$\mathbf{n_e}$	$\mathbf{n_e-n_o}$
LN	2.1416	2.0415	-0.1001	2.1313	2.0327	-0.0986
$Zr_{Li}^{3+}+Nb_{Li}^{4+}+7v_{Li}^{-}$	2.5259	2.4589	-0.0670	2.5055	2.4399	-0.0656
$Zr_{Li}^{3+}+3v_{Li}^{-}$	2.5051	2.3999	-0.1052	2.4863	2.3833	-0.1030
$Zr_{Li}^{3+}+3Zr_{Nb}^{-}$	2.4819	2.3456	-0.1363	2.4633	2.3299	-0.1334
$Zr_{Li}^{3+}+3Zr_{Nb}^{-}+3v_{Li}^{-}$	2.4799	2.4039	-0.0760	2.4620	2.3871	-0.0749